



Single Phase Eleven Level Grid Connected Inverter for Photovoltaic System

Veerla Usha Sri¹, Dr. Y Bhaskar S S Gupta M.Tech, Ph.D²

¹ Pg Student, Dept. of Electrical and Electronics Engineering, Vignan's Institute of Engineering For Women, Visakhapatnam, A.P – 530049.

² Associate Professor, Dept. of Electrical and Electronics Engineering, Vignan's Institute of Engineering for Women, Visakhapatnam, A.P – 530049.

ABSTRACT

The typical consumer or user of a single-phase grid-connected inverter is a small business or institution that requires a power range of less than 10 kW. Different kinds of single-phase inverters that can connect to the grid have been studied. With its high switching frequency, the three-level inverter can meet requirements, but at the expense of possibly higher switching losses, noise, and interference. The inverter's switching function generates electromagnetic interference (EMI), which can be mitigated by optimising the waveform it produces. For photovoltaic systems that link to the grid, this research presents a novel pulse width modulated (PWM) control strategy for a single-phase, seven-level inverter. The PWM signals were generated by comparing three identical reference signals with an offset equal to the amplitude of the triangle carrier signal. From the dc source voltage, the inverter may generate seven different levels of output-voltage levels (V_{dc} , $2V_{dc}/3$, $V_{dc}/3$, 0 , $V_{dc}/3$, $2V_{dc}/3$, V_{dc}). Multilevel inverters have cleaner output waveforms and reduced THD than single-stage inverters. Extensive MATLAB simulations were run to examine the proposed multilevel inverter's operation. The inverter's output voltage can be varied by setting the modulation index to the desired value. A comparison is made between the output of a 7-level inverter and that of an 11-level inverter.

KEYWORDS: PV System, MPPT, Boost Chopper, 11-level Inverter.

I. INTRODUCTION

As the world's energy needs continue to grow, the price of fossil fuels continues to rise, and the state of the environment continues to deteriorate, there has been a surge in interest in renewable energy generation systems like photovoltaic. The energy from the Sun is transformed into electricity by such a system. Grid-connected inverters transmit electricity generated by photovoltaic panels to the electrical grid. The typical usage of a single-phase grid-connected inverter is for low-power or domestic applications with power requirements of less than 10 kW. Different kinds of single-phase inverters that can connect to the grid have been studied. Full-bridge three-level architecture is widely used in this type of inverter. With its high switching frequency, the three-level inverter can meet requirements, but at the expense of possibly higher switching losses, noise, and interference. It is possible to lessen the amount of EMI produced by the inverter's switching activity and shrink the size of the filter by altering the shape of the output waveform. Multilevel inverters have a number

of advantages over traditional two-level inverters, including nearly sinusoidal output-voltage waveforms, a good harmonic profile for the current they produce, reduced strain on electronic components, lower switching losses, smaller filter sizes, and less electromagnetic interference. Numerous topologies for multilevel inverters have been created over time. Common types include diode-clamped, flying-capacitor/multi-cell, cascaded H-bridge, & modified H-bridge multi-level. A newly proposed H-bridge single-phase multilevel inverter with two diode-embedded bidirectional switches as well as a new pulse width modulation (PWM) technique is described in detail, along with its design, fabrication, and testing. Using a current-control algorithm and a maximum-power-point tracker, this architecture was applied to a photovoltaic (pv) system that was wired into the municipal electricity grid. To accomplish this, maximum power point tracking (MPPT) is used, and the results of the simulated implementation are reviewed.

II. PHOTOVOLTAIC SYSTEM

2.1 Photovoltaic Effect

In photovoltaics (PV), semiconductors that are susceptible to the photovoltaic effect are used to convert solar energy into direct current electricity.

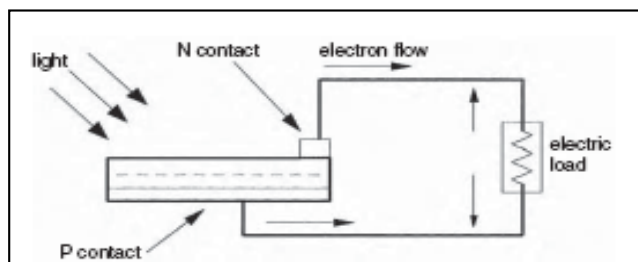


Fig 2.1: PV effect converts the photon energy into voltage across the p-n junction

Solar panels, made up of many individual cells, each of which contains a photovoltaic material, are used to generate electricity using photovoltaics. Silicon (both monocrystalline and polycrystalline), polysilicon, amorphous silicon, cadmium telluride, and copper indium selenide/sulfide are now employed as photovoltaic materials. Modern solar cell and photovoltaic array production has made great strides in recent years in response to the increasing demand for these clean energy technologies.

2.2 Equivalent Circuit

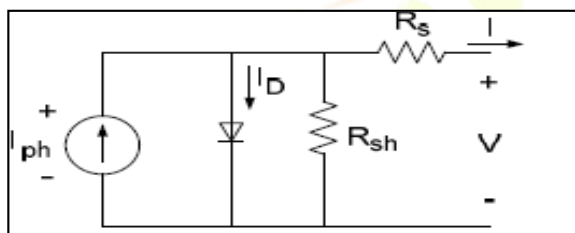


Fig 2.2 PV cell equivalent circuit

The PV cell's corresponding electrical circuit simplifies the cell's intricate physical workings. Here are the specifics of the circuit. A resistance that is applied in a sequence. It is the pn-junction depth, impurities, & contact resistance that determine R_s , the internal resistance to current flow. As the leakage current to ground increases, the shunt resistance R_{sh} decreases. There is no series loss when $R_s = 0$ and $R_{sh} = 0$ in a perfect PV cell (no leakage to ground). R_s ranges from 0.05 to 0.10 and R_{sh} from 200 to 300 in a typical high-quality silicon cell. Modifications to R_s have a noticeable impact on PV conversion efficiency, but modifications to R_{sh} have no effect. Increases in R_s , even by a little amount, can have a dramatic effect on PV output. Delivered current to the load is equal to the illumination current I_{ph} minus the diode current I_D as well as the shunt leakage current I_{sh} in the analogous circuit. If the load current is zero, or $I = 0$, then the cell's open-circuit voltage V_{oc} can be calculated as follows:

$$V_{oc} = V + IR_{sh}$$

The series resistance (R_s) is negligibly small compared to the shunt resistance (R_{sh}). To keep the solar cell model simple, these resistances are often ignored. Above is a diagram depicting the ideal voltage-current characteristics of a solar cell, which is provided by the relation below.

$$I = I_{ph} - I_D$$

$$I = I_{ph} - I_0$$

Where,

I_{ph} = Photocurrent,

I_D = Diode Current,

I_0 = Saturation Current,

A = Ideality Factor,

q = Electronic Charge = 1.6×10^{-19} ,

k_B = Boltzmann's gas constant = 1.38×10^{-23} ,

T = Cell Temperature,

R_s = Series Resistance,

R_{sh} = Shunt Resistance,

I = Cell Current,

V = Cell Voltage

The power output of a solar cell is given by

$$P_{PV} = V_{PV} * I_{PV}$$

Where,

I_{PV} = Output current of solar cell (A).

V_{PV} = Solar cell operating voltage (V).

P_{PV} = Output power of solar cell (W).

2.3 MPPT (Maximum Power Point Tracking)

Maximum power point

Is the operating point A (V_{max} , I_{max}) at which the power dissipated in the resistive load is maximum: $P_{max} = I_{max} * V_{max}$

Maximum efficiency

Maximum power density is the ratio of incident light density to the maximum power density. Modules and other PV devices are tested in real-world applications by subjecting them to controlled environments. Typically, the manufacturer's provided module characteristics are determined in a controlled environment. The maximum power wasted in a resistive load occurs at operating point A (V_{max} , I_{max}). Maximum power output is equal to maximum current multiplied by maximum voltage. At this precise moment, the greatest power that can be gathered by the MPPT is 1000wb/m². This allows us to boost the solar cell's output efficiency and response time (PV).

2.3.1 MPPT Algorithms

It is possible for maximum power point trackers to use multiple algorithms and toggle between them depending on the array's operational parameters. Different algorithms or approaches to MPPT are,

1. Constant Voltage
2. Short Circuit Current
3. Incremental Conductance
4. Perturb and Observe

2.3.2 Proposed MPPT Algorithm

Perturb and Observe, where the current is regulated, is the MPPT algorithm suggested. Typically, the designer can alter either the PV voltage or current. Figure 2.3 demonstrates how VMP variations are proportional to Ln(irradiance), and Figure 2.4 demonstrates how IMP is also light intensity dependent.

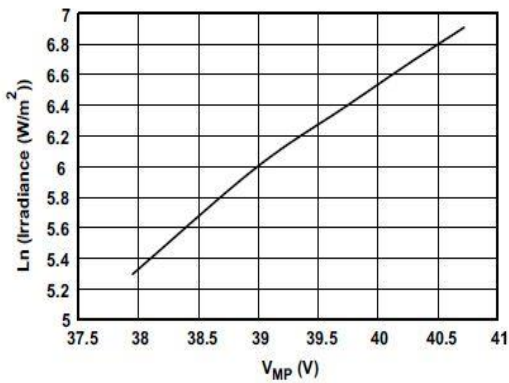


Figure 2.3 Irradiance vs V_{MP} for 200 to 1000 W/m^2

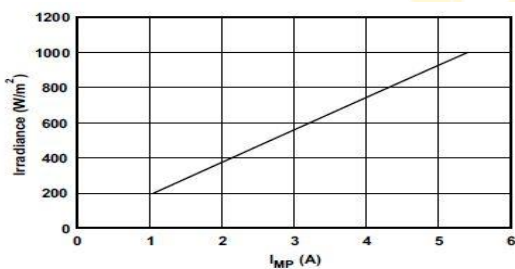


Figure 2.4 Irradiance vs I_{MP} for 200 to 1000 W/m^2

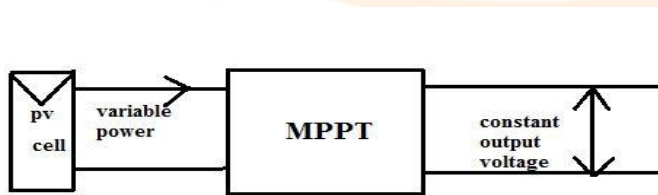


Fig 2.6 Block diagram of P&O Algorithm

III. STEP-UP CHOPPER/ BOOST CHOPPER

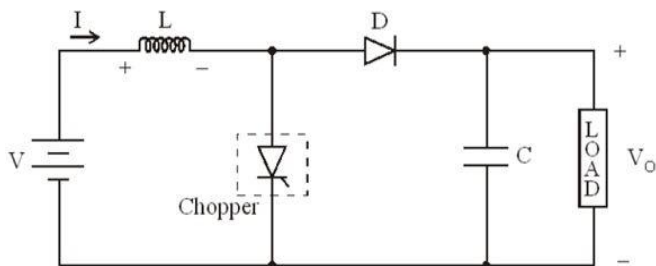


Fig 3.1 Step-Up Chopper/Boost Chopper

A step-up chopper, depicted in Figure 3.1, converts the lower input voltage V into a greater output voltage V_o . Each application has different needs for output voltage and current, which guides the selection of appropriate values for L and C . As long as the chopper is switched on, inductor L will be linked across the power source. Whenever the ON tie of a chopper, T_{on} , is present, the inductor's current, I , increases and it saves energy. Chopping off power for a time period T_{off} causes the inductor current I to pass through the diode D & load. As the current drops, the induced

EMF in L flips its polarity. Thus, the load voltage is calculated as

$$V_o = V + L \frac{di}{dt} \text{ i.e., } V_o > V$$

The thyristor is utilized as a toggle in the circuit. Whenever the thyristor is active, supply voltage is observed all across load, and when it is disabled, there is no voltage all across load. The following diagram illustrates a step-up or pulse-width-modulated (PWM) boost converter. Elements included the dc input voltage source (V_S), a boost inductor (L), a controlled switch (S), a diode (D), a filter capacitor (C), as well as a load resistance (R). The waveforms employed by the converters in the CCM are presented in Fig. Whenever switch S is actuated, diode D is turned off, then current through the boost inductor increases in a linear pace. Whenever the switch S is turned off, the inductor's conserved energy is transmitted to the chosen load via diode (R -Load) (R -Load).

IV. INVERTERS

4.1 Introduction to Inverters

In order to convert low-voltage direct current (D.C.) energy into standard-voltage alternating current (A.C.) for usage in homes and businesses, electrical devices called D.C.-A.C. inverters are employed. This makes them ideal for situations where standard AC mains power is unavailable but electric tools and appliances must be used. Caravan and mobile home appliance use, as well as the use of audio, video, and computer equipment in outlying locations, are all examples. Most inverters accomplish their goals by first transforming the input direct current (D.C.) into alternating current (A.C.), and then increasing the output A.C.'s voltage to the level of the utility grid using a transformer. The designer's aim is for the inverter to carry out these tasks with minimal loss of energy as heat, converting as much of the DC current from the battery / solar panel as feasible to AC current for the building's mains.

4.2 Proposed Multilevel Inverter Topology

The proposed single-phase seven-level inverter builds on a base of a five-level inverter by adding an extra two stages. The circuit consists of a single-phase conventional H-bridge inverter, two bidirectional switches, a capacitor voltage divider with components C_1 , C_2 , and C_3 , and the three capacitors. The modified H-bridge topology provides many advantages over other topologies for inverters with the same number of levels, such as the ability to employ a smaller power switch, power diodes, as well as capacitors. Connecting the Solar panels to the inverter required a dc-dc boost converter. Since the inverter's output will be connected directly to the utility grid rather than a load, this is the method that was used. The voltage from the PV arrays was less than the voltage from the grid, so a DC-DC boost converter was required. High dc bus voltages are required for power export from Photovoltaic panels to the grid. Using inductance L_f as a filter, the injected current was cleaned up before being sent back into the grid. The inverter's switches allow for seven distinct output voltage levels, depending on the dc

source voltage: V_{dc} , $2V_{dc}/3$, $V_{dc}/3$, $0V_{dc}$, $2V_{dc}/3$, $V_{dc}/3$. The operation of the proposed inverter can be divided into seven different switching states (shown in Fig. 4.1–4.7).

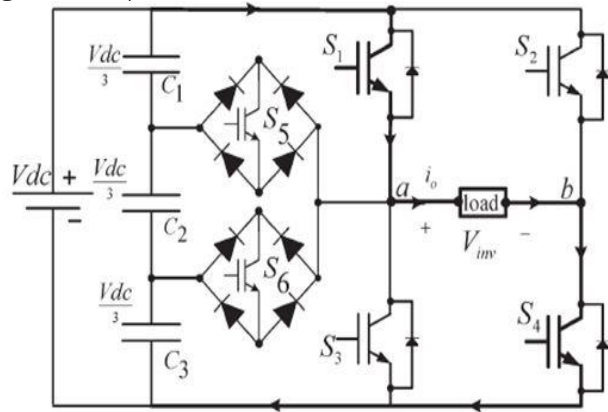


Fig 4.1 Inverter circuit for the output voltage (V_{dc})

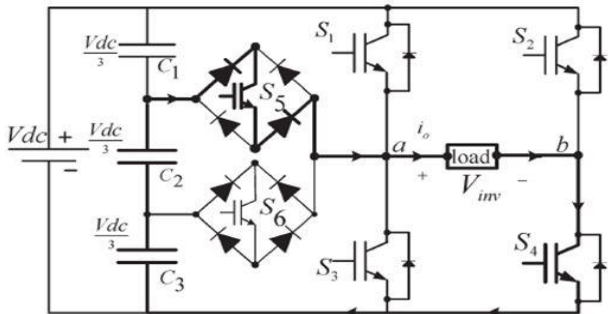


Fig 4.2 Inverter circuit for the output voltage ($2V_{dc}/3$)

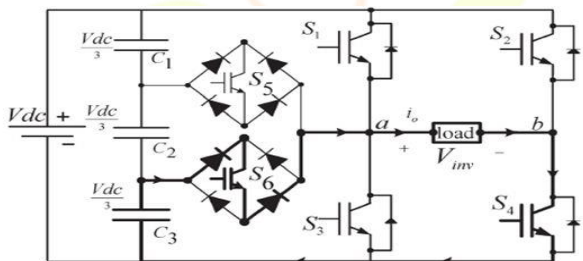


Fig 4.3 Inverter circuit for the output voltage ($V_{dc}/3$)

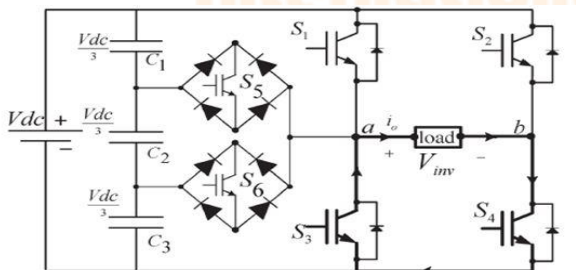


Fig 4.4 Inverter circuit for the output voltage (zero 0)

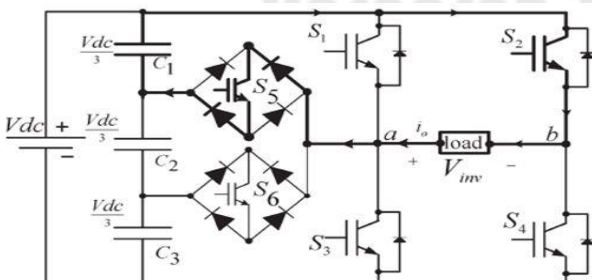


Fig 4.5 Inverter circuit for the output voltage ($-V_{dc}/3$)

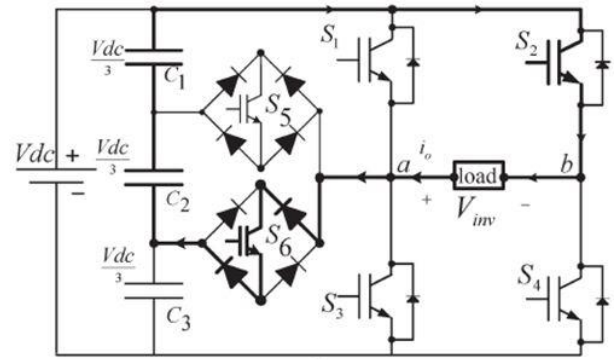


Fig 4.6 Inverter circuit for the output voltage ($-2V_{dc}/3$)

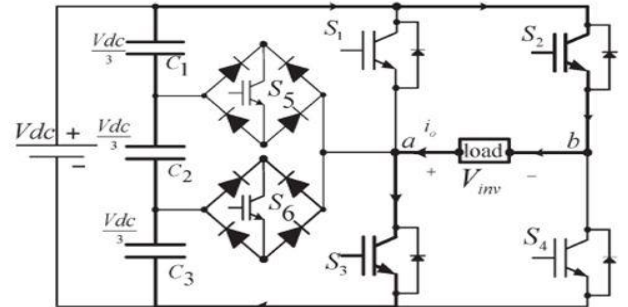


Fig 4.7 Inverter circuit for the output voltage ($-V_{dc}$)

Table 4.1 Output voltage according to the switches on-off condition

v_0	S_1	S_2	S_3	S_4	S_5	S_6
V_{dc}	on	off	off	on	off	off
$2V_{dc}/3$	off	off	off	on	on	off
$V_{dc}/3$	off	off	off	on	off	on
0	off	off	on	on	off	off
0^*	on	on	off	off	off	off
$-V_{dc}/3$	off	on	off	off	on	off
$-2V_{dc}/3$	off	on	off	off	off	on
$-V_{dc}$	off	on	on	off	off	off

Table shows the switching combinations that generated the seven output-voltage levels (0 , $-V_{dc}$, $-2V_{dc}/3$, $-V_{dc}/3$, V_{dc} , $2V_{dc}/3$, $V_{dc}/3$).

V. CONTROL STRATEGY

5.1 Introduction

A Maximum Power Point Tracking (MPPT) algorithm, dc-bus voltage controller, reference-current generator, and current controller are all shown in Figure 5.1 as part of the control system. The key objectives of control system are to maximise the energy transfer from the Photovoltaic panels to the grid and to generate a sinusoidal current having minimal harmonic distortion even while taking into consideration harmonics with in grid voltage. Because of its straightforward design and minimal dependence on externally observable parameters, the perturb-and-observe (P&O) algorithm is implemented in the proposed inverter for use in MPPT. It does this by periodically changing the terminal voltage of the array by an amount (either up or down) and comparing the PV output power to the power output during the previous cycle of perturbation. In the next cycle, the perturbation would move in the same direction if the power was increasing, but it would reverse if the power was decreasing. This implies that the terminal voltage of the array is changed at regular

intervals during MPPT cycles, causing the P&O algorithm to bounce around the MPP once it is reached. A dc-dc boost converter using the P&O algorithm was built. The duty-cycle function is the output of the MPPT. The duty cycle of the AC-DC seven level PWM inverter determines the voltage at the PV panels' output by regulating the dc-link voltage V_{dc} . The DC-DC boost converter's output voltage (V_{dc}) is maintained by a PID controller, which compares V_{dc} to V_{dcref} and uses the error to regulate the output voltage. Keeping the V_{dc} constant and above 2 of V_{load} ensures that power is consistently supplied to the load. Power from a PV inverter may only be sent to the grid if its frequency and phase are synchronised with those of the grid. Reference current generation is dependent on synchronising the sine lookup table with the grid voltage (V_{load}). This requires determining the grid's period and phase. In this section, the entire response is managed; several PID controllers are used to generate the sinusoidal signal; the sine lookup table and the zero crossing detector are utilised for the latter. Under closed loop conditions, the complete reaction is regulated to get precise results.

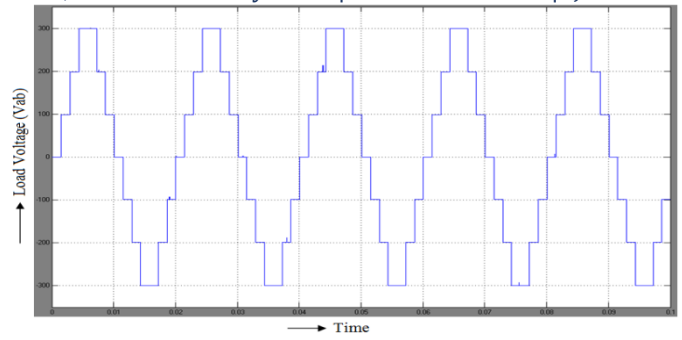


Fig 6.2 Seven levels of Inverter output voltage (V_{inv})

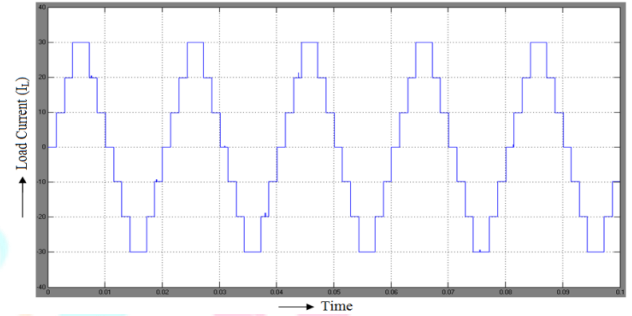


Fig 6.3 Seven levels of Inverter output current (I_{inv})

For $R=10\Omega$

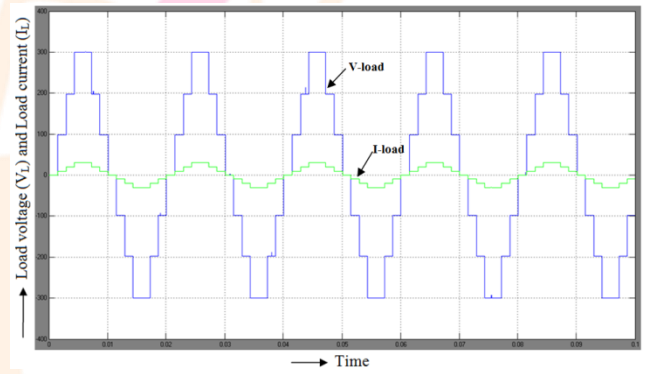


Fig 6.4 Load voltage (V_{Load}) and Load current (I_{Load}) that are in phase

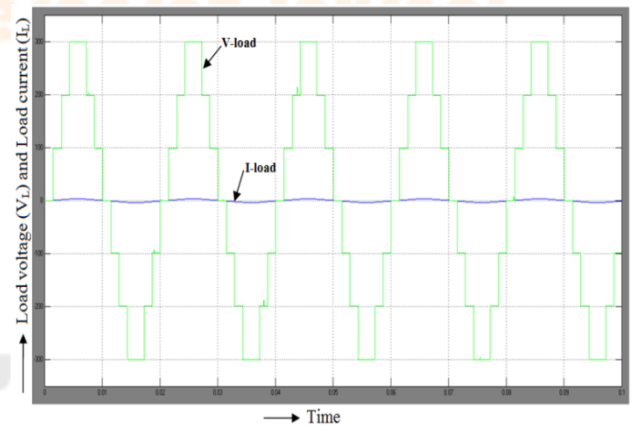


Fig 6.5 Load voltage (V_{Load}) and Load current (I_{Load}) that are in phase

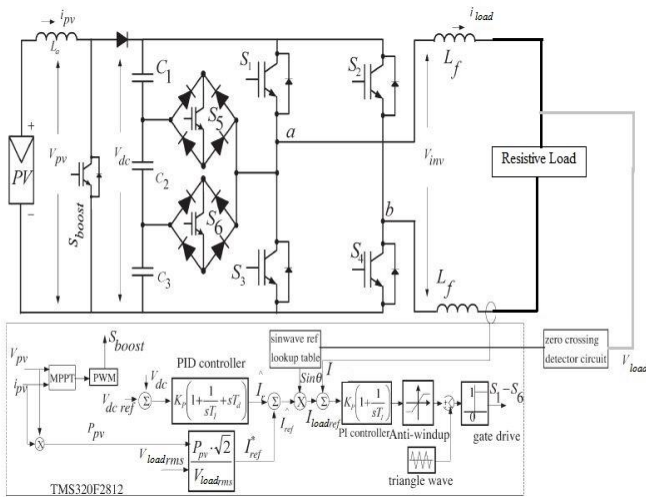


Fig. 5.1 Seven-level inverter with closed-loop control algorithm

VI. SIMULATION RESULTS

6.1 Block Diagrams

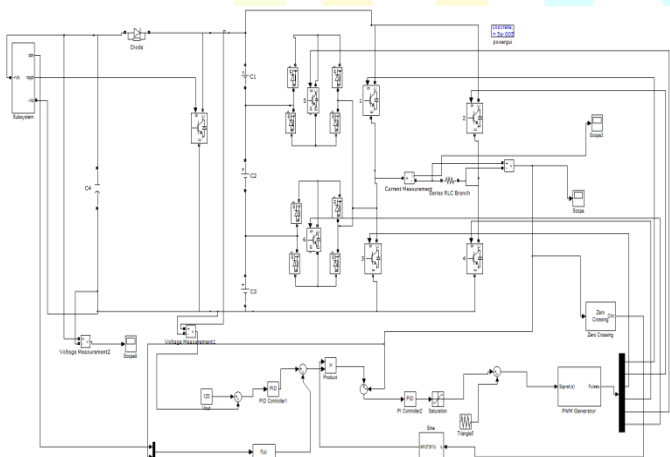


Fig 6.1 Main MATLAB/Simulink Seven level Inverter Block diagram

6.2 Simulation Results

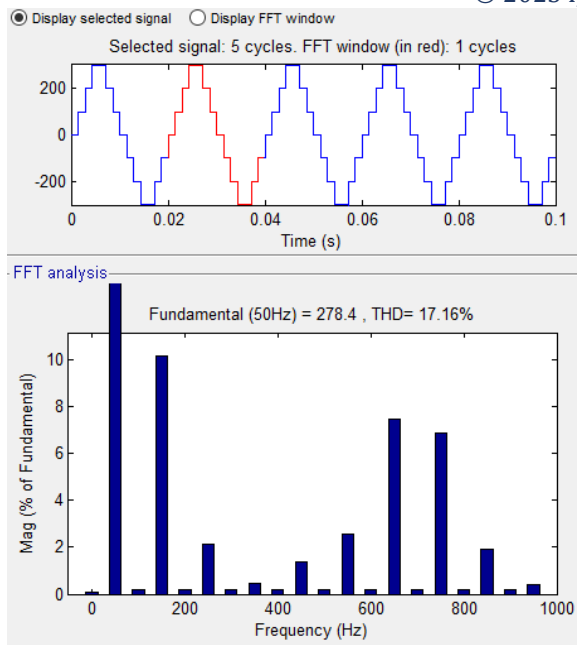


Fig. 6.6. THD for seven level inverter

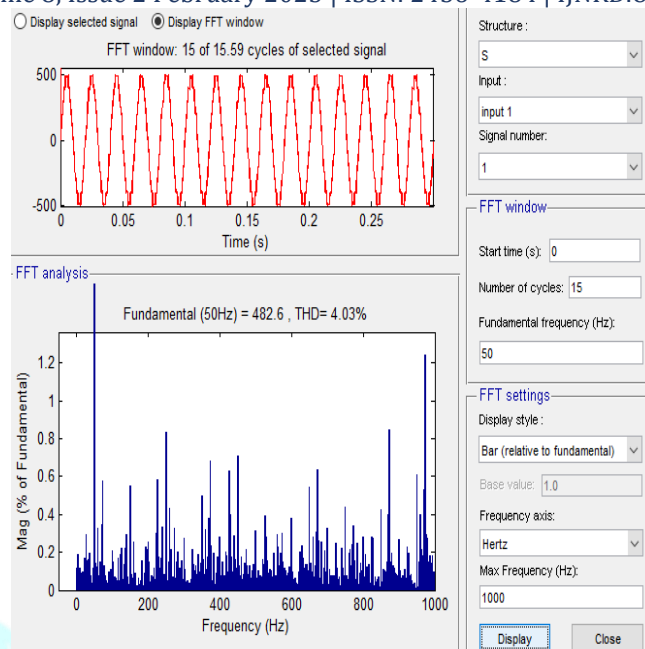


Fig. 6.9. THD for Eleven level inverter

6.3 Eleven Level Simulation

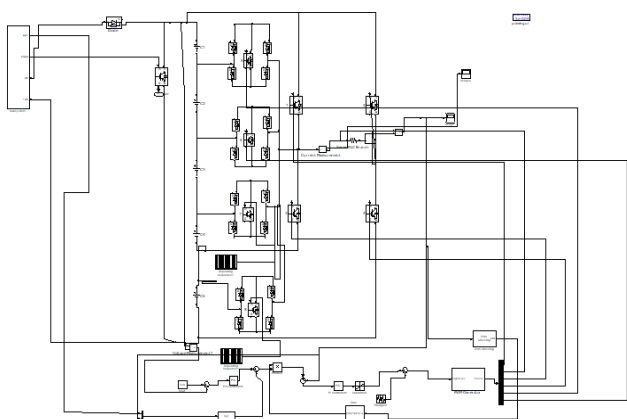


Fig 6.7 Main MATLAB/Simulink Eleven level Inverter Block diagram

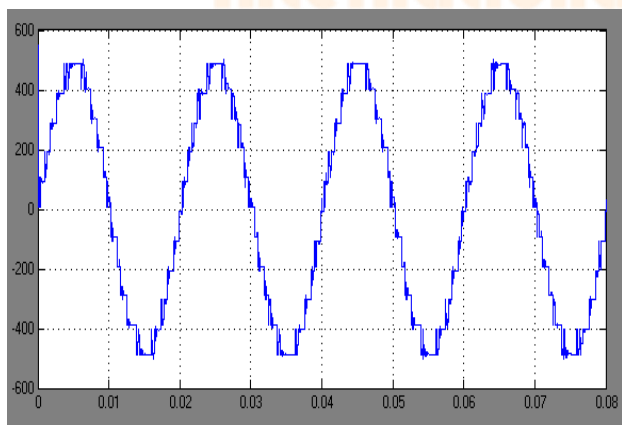


Fig 6.8 Eleven levels of Inverter output voltage (V_{inv})

VII.CONCLUSIONS

An innovative PWM switching technique for the suggested multilevel inverter has been given in this study. It creates PWM switching signals by using three reference signals as well as a triangle carrier signal. The proposed multilevel inverter's operation was thoroughly investigated. The inverter's output voltage can be varied by setting the modulation index to the desired value. Eleven level inverter is used to evaluate the findings. The seven-level inverter's reduced total harmonic distortion (THD) makes it a desirable option for grid-connected PV inverters. This seven-level inverter allows for fewer switching states and more stable operation, improving the system's overall response. The total harmonic distortion (THD) achieved from an eleven-level inverter is less than that from a seven-level inverter.

REFERENCES

- [1] Nasrudin A. Rahim, Jeyraj Selvaraj, "Single-Phase Seven-Level Grid-Connected Inverter for Photovoltaic System", *IEEE Trns. on industrial electronics*, VOL. 58, NO. 6, JUNE 2011.
- [2] S. B. Kjaer, J. K. Pedersen, and F. Blaabjerg, "A review of single-phase grid connected inverters for photovoltaic modules," *IEEE Trans. Ind.Appl.*, vol. 41, no. 5, pp. 1292–1306, Sep./Oct. 2005.
- [3] J. Rodriguez, J. S. Lai, and F. Z. Peng, "Multilevel inverters: A survey of topologies, controls, and applications," *IEEE Trans. Ind. Electron.*, vol. 49, no. 4, pp. 724–738, Aug. 2002.
- [4] J. Selvaraj and N. A. Rahim, "Multilevel inverter for grid-connected PV system employing digital PI controller," *IEEE Trans. Ind. Electron.*, vol. 56, no. 1, pp. 149–158, Jan. 2009.
- [5] Dinesh, L., Sesham, H., & Manoj, V. (2012, December). Simulation of D-Statcom with hysteresis current controller for harmonic reduction. In *2012 International Conference on Emerging Trends in Electrical Engineering and Energy Management (ICETEEEM)* (pp. 104-108). IEEE
- [6] J. Huang and K. A. Corzine, "Extended operation of flying capacitor multilevel inverter," *IEEE Trans. Power Electron.*, vol. 21, no. 1, pp. 140–147, Jan. 2006.
- [7] Manoj, V. (2016). Sensorless Control of Induction Motor Based on Model Reference Adaptive System

(MRAS). *International Journal For Research In Electronics & Electrical Engineering*, 2(5), 01-06.

- [8] J. I. Leon, S. Vazquez, S. Kouro, L. G. Franquelo, J. M. Carrasco, and J. Rodriguez, "Unidimensional modulation technique for cascaded multilevel converters," *IEEE Trans. Ind. Electron.*, vol. 49, no. 5, pp. 1058-1064, Oct. 2002.
- [9] V. B. Venkateswaran and V. Manoj, "State estimation of power system containing FACTS Controller and PMU," 2015 IEEE 9th International Conference on Intelligent Systems and Control (ISCO), 2015, pp. 1-6, doi: 10.1109/ISCO.2015.7282281.
- [10] Manohar, K., Durga, B., Manoj, V., & Chaitanya, D. K. (2011). Design Of Fuzzy Logic Controller In DC Link To Reduce Switching Losses In VSC Using MATLAB-SIMULINK. *Journal Of Research in Recent Trends*.
- [11] Manoj, V., Manohar, K., & Prasad, B. D. (2012). Reduction of switching losses in VSC using DC link fuzzy logic controller *Innovative Systems Design and Engineering* ISSN, 2222-1727.
- [12] G. Ceglia, V. Guzman, C. Sanchez, F. Ibanez, J. Walter, and M. I. Gimenez, "A new simplified multilevel inverter topology for DC-AC conversion," *IEEE Trans. Power Electron.*, vol. 21, no. 5, pp. 1311-1319, Sep. 2006.
- [13] N. A. Rahim and J. Selvaraj, "Multi-string five-level inverter with novel PWM control scheme for PV application," *IEEE Trans. Ind. Electron.*, vol. 57, no. 6, pp.2111-2121, Jun. 2010.
- [14] Dinesh, L., Harish, S., & Manoj, V. (2015). Simulation of UPQC-IG with adaptive neuro fuzzy controller (ANFIS) for power quality improvement. *Int J Electr Eng*, 10, 249-268.
- [15] E. Villanueva, P. Correa, J. Rodriguez, and M. Pacas, "Control of a single phase cascaded H-bridge multilevel inverter for grid-connected photovoltaic systems," *IEEE Trans. Ind. Electron.*, vol. 56, no. 11, pp. 4399-4406, Nov. 2009.
- [16] "Modeling and Simulation of Photovoltaic module using MATLAB/Simulink", *International Journal of Chemical and Environmental Engineering*, Volume 2, No.5, October 2011.

